PNAS
www.pnas.org

Supplementary Information for

Ribosome collisions alter frameshifting at translational reprogramming motifs in bacterial mRNAs

Angela M. Smith[1], Michael S. Costello[1], Andrew H. Kettring[1], Robert J. Wingo[1], and Sean D. Moore[1]*

Sean D. Moore
Email: sean.moore@ucf.edu

This PDF file includes:

Supplementary text
Figures S1 to S6
SI References

Other supplementary materials for this manuscript include the following:

n/a

www.pnas.org/cgi/doi/10.1073/pnas.1910613116

Ribosome engagement at the 5' end of mRNAs

With certain mRNAs, there are mechanisms to initiate translation at the extreme 5’ ends of messages (1). Although these translation initiations require an AUG codon at the 5’ end in *E. coli* (2, 3), which our constructs lacked, we considered the remote possibility that some ribosomes may have engaged the 5’ ends of our reporter and mechanically traversed the untranslated region (for example, EF-G is stimulated by free ribosomes) (4). Such an event would have positioned trailing ribosomes behind the engaged reporter ribosomes and potentially impacted our experimental readout. To eliminate this possibility, we generated a variant of the reporter that was missing the majority of the untranslated leader, leaving only five nucleotides upstream of the SD sequence.

Ribosome rescue during stalling

Bacterial mRNAs are processively degraded from their 3' ends (5), so stalling amplifies an inherent physiological challenge because more ribosomes will inevitably read to the ends of mRNAs without encountering a stop codon and without completing their protein synthesis missions. To counter this problem, bacteria contain essential rescue factors that recycle ribosomes in this scenario by either recruiting tmRNA for *trans*-translation, using ArfA to activate RF2, or allowing ArfB to promote hydrolysis of the peptidyl-tRNA (6). Each of these systems require ribosomes with empty mRNA entry channels, which was not the case in our test systems. Moreover, normal reporter mRNA turnover and subsequent rescue by tmRNA would have led to the degradation of both the downstream mRNAs and nascent proteins in our systems.

Detailed Materials and Methods:

Culturing and Plasmid Construction - Overnight cultures were diluted 1:100 in MOPS EZ rich defined medium (Teknova, Hollister, CA) supplemented with 10 mM sodium bicarbonate, 0.2 % glycerol, and 0.002% glucose and grown to early exponential phase at 37 °C before reporter induction with 0.5 mM IPTG. Reporter plasmids and the SecM traps were constructed using derivatives of pTrc99a (7). Assembly of reporter backbones was accomplished using Gibson assembly (NEBuilder® HiFi, New England Biolabs, Ipswich, MA). Alterations to reporters were performed using ‘round-the-horn site-directed mutagenesis (8). Altered SD sequences were generated using a primer containing two random residues in the SD sequence and subsequent clones were screened for expression levels using Western blots.

Cell harvest and lysis - Frozen cubes of polysome cell wash buffer (25 mM HEPES-Tris, 150 mM NaCl, 20 mM MgOAc, pH 7.6) were crushed to fine pieces using a manual ice grinder and ~20 mL transferred to 50 mL conical tubes that were subsequently stored at -80 °C. 30 mL of cultures, grown at 37 °C, was poured over the -80 °C ice and cells were harvested by centrifugation at 4 °C. Cells were washed once in 10 mL ice cold polysome cell wash buffer, resuspended in 500 µL HT-20 lysis buffer (25 mM HEPES-Tris, pH 7.6, 100 mM K^+-glutamate, 20 mM MgAOc, 14 mM 2-mercaptoethanol, supplemented with Protease Inhibitor Cocktail Set V from Millipore Sigma) and transferred to ice-cold 2 mL screw cap tubes containing ~100 µL zirconium beads (0.1 mm, Research Products International, Mount Prospect, IL). Cells were lysed by bead ablation (MPBio FastPrep-24 5G, "*Escherischia coli* cells" setting), cell debris and beads

were removed by centrifugation and the cleared supernatant was transferred to clean tubes on ice.

Sucrose gradient fractionation - 10-40 % sucrose gradients in HT-20 buffer supplemented with 0.05 % Tween-20 were prepared in Beckman SW-41 centrifuge tubes (Seton Scientific, Petaluma, CA) using a Gradient Master™ instrument (BioComp Instruments, Fredericton, NB) and chilled to 4 °C. 200 µL of clarified lysate was loaded onto gradients and centrifuged in a Beckman SW-41 Ti rotor for 3.5 hours at 35,000 RPM (151,000 average RCF) at 4 °C. Gradients were fractionated and absorbance was recorded using a Piston Gradient Fractionator™ (BioComp).

Western blots and luminescence assays - Cultures were grown in MOPS EZ rich defined medium, induced with IPTG, chilled in an ice bath, quantified by turbidity at 600 nm, and normalized by harvesting differential volumes. For SDS-PAGE and Western blots, cells were resuspended directly in SDS loading buffer and incubated at 80 °C for 5 minutes prior to loading or storage. SDS-PAGE was performed using MES-Tris buffered gels (9) and proteins transferred to PVDF membrane (SigmaMillipore). Epitopes were detected using either anti-His_6 (A7058, SigmaMillipore) or anti-FLAG (A8592, SigmaMillipore) peroxidase-conjugated antibodies and reacted for luminescence using SuperSignal™ West Pico PLUS chemiluminescent substrate (ThermoFisher) prior to imaging using a FluorChem™ E system with Digital Darkroom software (ProteinSimple, San Jose, CA).

For luminescence measurements, iced cultures were normalized using growth medium in fresh tubes. Intracellular levels of NanoLuc were measured by mixing 40 µL of cells with 40 µL of Nano-Glo® Luciferase Assay System reagent according to the manufacturer's instructions (Promega, Madison, WI). Images of reaction wells were acquired using a FluorChem™ E (ProteinSimple) and luminescence signals were measured over time to monitor signal stability using a SpectraMax i3x microplate reader (Molecular Devices, San Jose, CA).

Template preparation for in vitro translation assays - The dual-luciferase mRNA transcript was generated from a PCR product template using an RNA synthesis kit (HiScribe™ T7 High Yield, New England Biolabs, Ipswich, MA). After synthesis for 3h at 37 °C, DNA was degraded by adding TURBO™ DNase (Invitrogen, Waltham, MA) and incubating for 15 min. RNA was extracted with phenol/chloroform/isoamyl alcohol (125:24:1, pH 4.3, Thermo Fisher). Following an additional extraction with chloroform to remove residual phenol, potassium acetate was added to 300 mM and samples were precipitated with an equal volume of 95 % ethanol, washed with 75 % then 95 % ethanol, dried, and resuspended in RNA buffer (10 mM bis-Tris, 0.1 mM EDTA, pH 6.5). RNA integrity was confirmed using UREA-PAGE followed by staining with Sybr Green II (Sigma-Aldrich) and quantified by absorbance at 260 nm.

Purification of nascent peptides for mass spectroscopy - 50 mL cultures containing the SecM-stall plasmid were induced in exponential phase for 20 min before being iced, harvested, washed, and lysed in 250 µL of HT-12 as described above. Sucrose gradient polysome fractions were diluted 10-fold into a mildly alkaline, denaturing buffer (25 mM Tris-Cl, 6 M guanidine-Cl, 14 mM 2-mercaptoethanol, 0.05 % Tween-20; pH 8.8). 50 µL of Ni-NTA resin was added (Thermo Fisher Scientific, Waltham, MA), and the mixture incubated at room temperature for 1 h to allow for peptidyl-tRNA hydrolysis and Ni^{++} binding. His_6-containing peptides were eluted with HT-12 containing 300 mM imidazole, desalted using C_{18} ZipTips (MilliporeSigma, Burlington, MA), and eluted in 80%

acetonitrile with 0.1 % trifluoroacetic acid. Peptides were embedded in α-cyano-4-hydroxycinnamic acid (MilliporeSigma) for analysis in a Microflex MALDI-TOF spectrometer (Bruker Daltonics, Billerica, MA). Spectral data were processed using Mmass 5 (10).

Preparing qPCR templates - RNA was purified from sucrose gradients by mixing 200 µL of 5 M guanidine thiocyanate and 3 µL of 10 mg/mL linear polyacrylamide into ~450 µL of selected fractions prior to extraction with phenol/chloroform as described above. Residual DNA was degraded using TURBO™ DNase followed by a second phenol extraction and ethanol precipitation. RNA samples within an experimental set were normalized to each other using 260 nm absorbance and mixed with target antisense primer pools (100 nM each final) prior to unfolding and annealing (from 95 to 22 °C over 25 min). Reverse transcription of 3 µL of each mixture was carried out using the iScript™ Select cDNA Synthesis Kit (Bio-Rad, Hercules, CA) and then diluted 5-fold with dH_2O prior to qPCR.

Western blot band integrations - Digital images were processed using ImageJ software (11) and data exported to Excel (Microsoft, Redmond, WA) and/or Prism (GraphPad Software, San Diego, CA) for processing and plotting. Statistical calculations of standard deviations and *t*-test P-values were calculated using Excel or Prism. Figure images were constructed using Illustrator (Adobe Systems, San Jose, CA).

Global fitting of RT-qPCR data - The published RT-qPCR analysis method was redeveloped with a limited user web interface and hosted at http://www.bioinformatics.org/ucfqpcr (Scilico, LLC). An open-source development version of the global fitting algorithm termed qPyCR was written for this project in Python (www.python.org) that improved fitting performance and allowed for the export of fitting statistics. A project description and Linux version that can run on Apple OSX is available at http://bioinformatics.org/qpycr/wiki/.

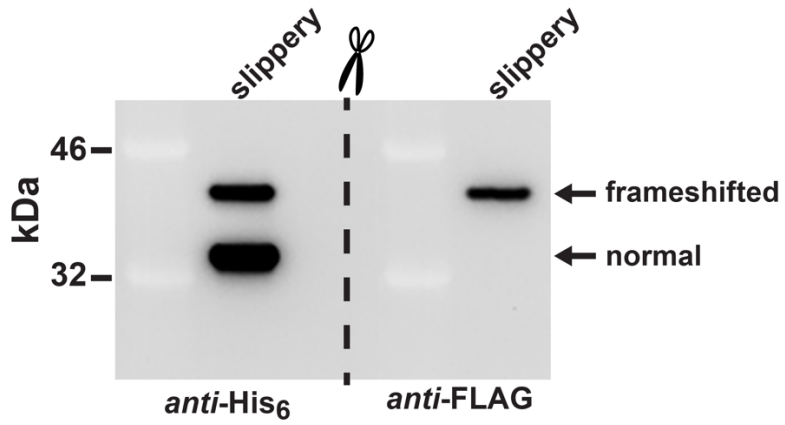

Fig. S1. The frameshifted product contains a FLAG epitope. The *IS3* frameshift reporter was analyzed using Western blots to evaluate the epitopes present. A gel was run with duplicate loads of molecular weight marker (*kDa*) and a total cell lysate containing the reporter with the *slippery IS3* motif. After electrophoresis and transfer, the membrane was cut and each half was evaluated using either *anti*-His_6 or *anti*-FLAG antibodies. The sections were then re-aligned prior to imaging. The locations of the *normal* and *frameshifted* products are indicated.

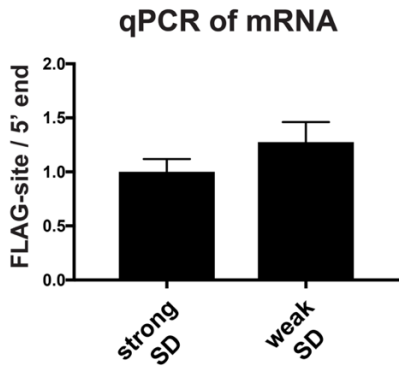

Fig. S2. Abundance of mRNA past the test region. Total RNA was extracted from cultures expressing either the *strong* or the *weak IS3* frameshift reporter and converted to cDNA prior to real-time qPCR. The qPCR seed values were calculated for each set and the ratio of the signals from just past the FLAG encoding region in the mRNA was divided by the signals from the 5' ends of the reporters. The ratios were then normalized to the value from the *strong SD* reporter mRNA. Error bars represent the deviations, accounting for error propagation during division, from three replicate measurements.

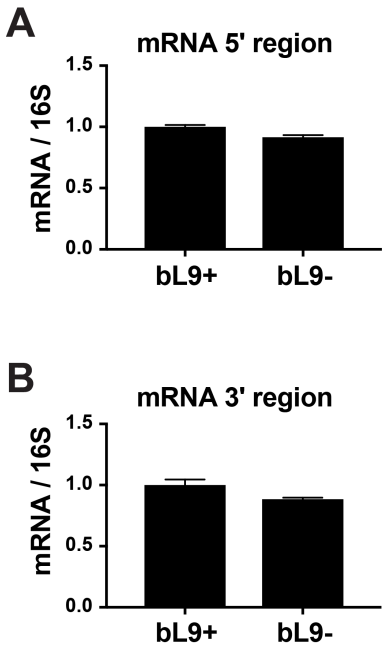

Fig. S3. Non-collision reporter mRNA levels. Total RNA was extracted from the cultures whose luminescence was presented in Fig. 7 and converted to cDNA prior to qPCR analyses. **A)** The ratio of qPCR signals derived from amplification of the 5' region of the reporter was compared to the signals from the 5' region of 16S rRNA. **B)** The ratio of qPCR signals derived from amplification of the 3' region of the reporter was compared to the signals from the 5' region of 16S rRNA. Error bars represent the deviations, accounting for error propagation during division, from three replicate measurements.

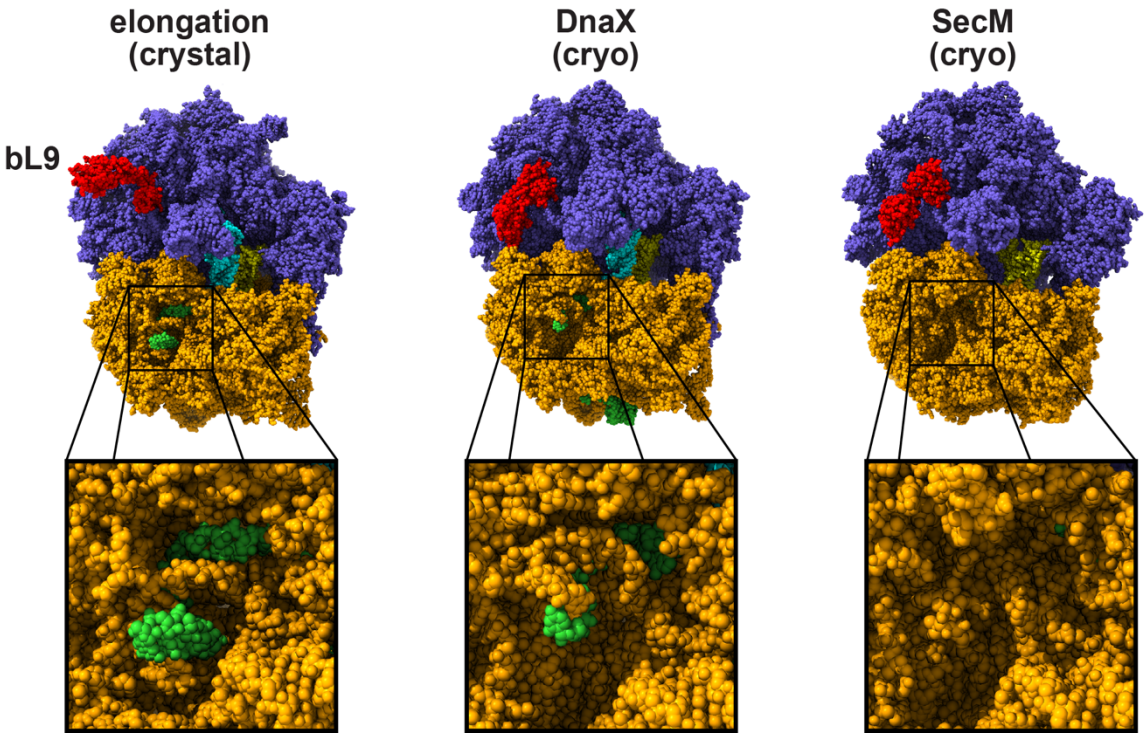

Fig. S4. Exit sites of ribosomes containing mRNAs. Representative structures of ribosomes were rendered to observe their tRNA E-sites and mRNA exit sites with their uL1 stalks centered toward the viewer. The expanded views show the mRNA exit regions in greater detail to show the variable positioning of the SD:anti-SD helix and that mRNA is unresolved (dynamic) in the absence of that interaction. The 50S subunits are colored *slate*, the 30S subunits are *orange*, protein bL9 is *red*, E-site tRNAs are *cyan*, P-site tRNAs are *yellow*, and mRNAs are *lime green*. The *elongation (crystal)* was rendered using PDB 4v6f (12), the *DnaX (cryo)* was rendered using PDB 5uq7 (13), and the *SecM (cryo)* was rendered using PDB 3jbu (14).

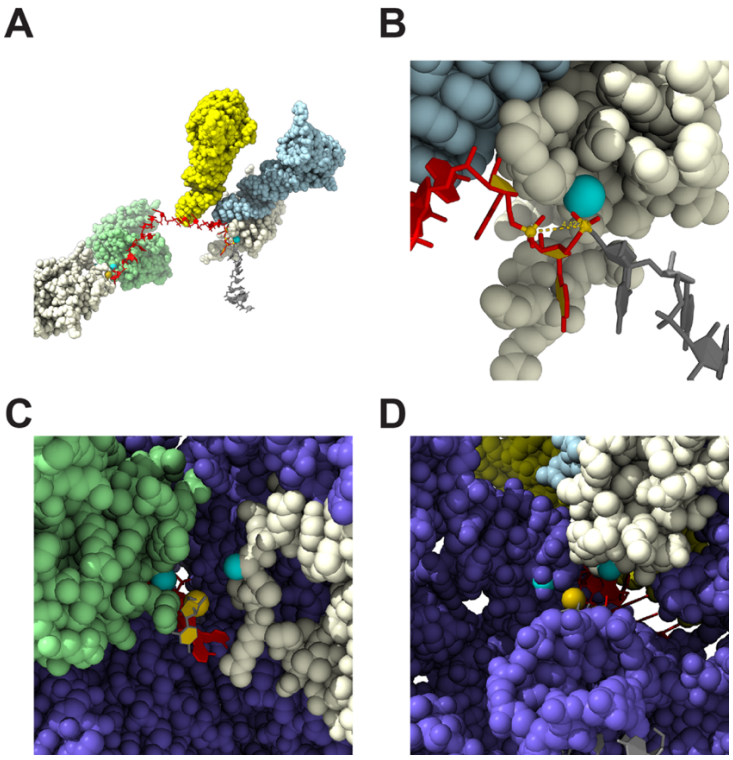

Fig. S5. Establishing location proxies for mRNA entrance and exit sites. A cryo-EM structure of the *T. thermophilus* ribosome engaged with a *dnaX* motif at 3.5 Å resolution (PDB 5uq7) (13) was used to establish an approximate length of an elongated codon and to identify adjacent atoms in the ribosome to be used as proxies for measuring mRNA exit-to-entrance distances in modeled collision complexes using different ribosome structure data sets. **A)** A rendering of the mRNA (*red* and *grey*), P-site (*yellow*) and E-site (*light blue*) tRNAs, uS3 (*light green*), uS4 (*light yellow*), and uS7 (*light grey*). Groups of three-nucleotide sets in the mRNA were measured from their 5' phosphorus (P) to their 3' oxygen (O) atoms and the lengths of the five longest groups were averaged to establish an extended codon length of 15.99 +/- 0.81 Å. **B)** The mRNA exit position was designated as the position of the 5' P of the nucleotide preceding the E-site codon. This atom is ~4.4 Å away from the 5' P of the first nucleotide of the E-site codon (*yellow* distance marker). The atomic proxy for this position in uS7 was the gamma carbon in Val80 (*cyan*), which is positioned orthogonally to the direction of exiting mRNA. **C)** Closeup view of the mRNA entrance channel. The 5' P of the first exposed nucleotide (the 7th from the A-site codon, residue C26 in this mRNA) is colored *gold* and the orthogonal distance proxy atoms are *cyan* (the beta carbon in Ala129 of uS3 and the beta carbon of Arg47 in uS4). These atoms were selected because they are slightly above this mRNA and represent the orthogonal position when the entrance channel is more tightly closed, which is observed in some structures (12). **D)** View of the mRNA exit site with the reference mRNA P atom in *gold* and the distance proxies in *cyan* (5' P of G693 of the 16S rRNA and gamma carbon of Val80 in uS7). Overall, these reference positions established 16 nucleotides within the ribosome.

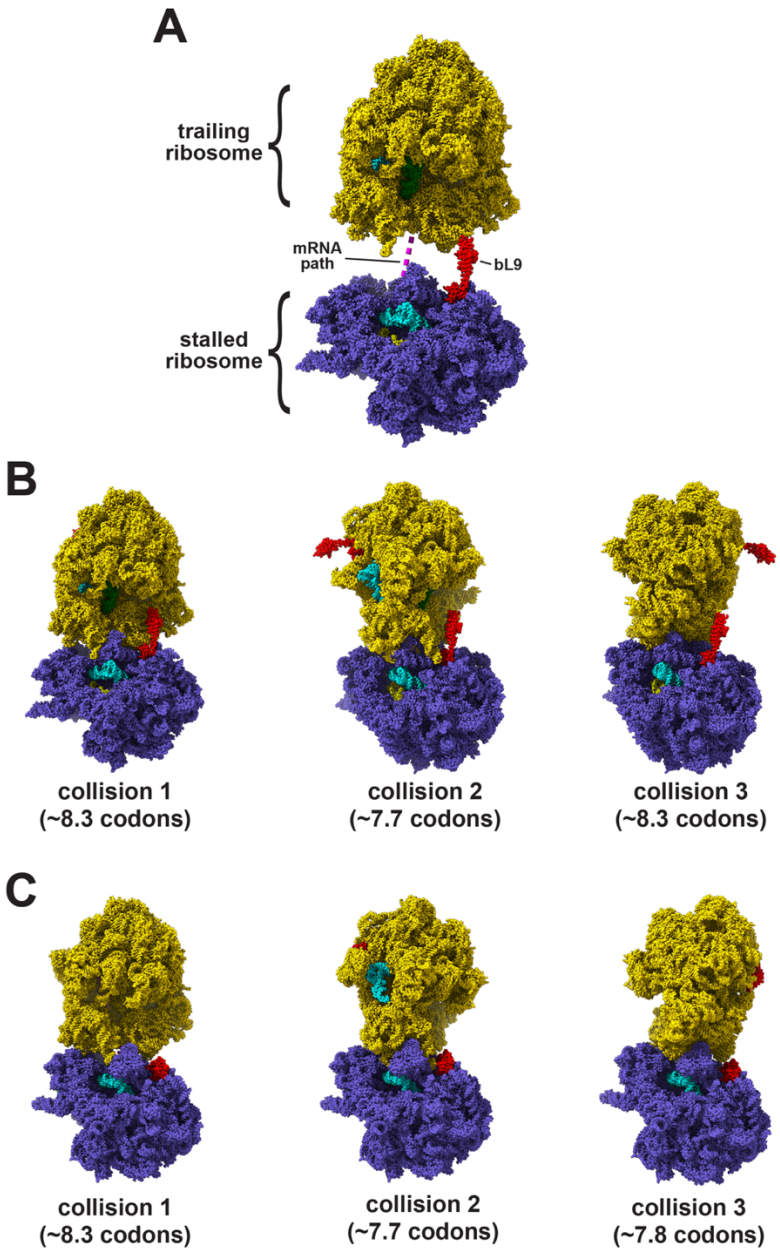

Fig. S3. Modeling ribosome collision complexes. The distances between mRNA exit and entrance sites were measured using the atom proxies described in Fig. S5. **A)** Example of separated particles from a crystal structure of *T. thermophilus* ribosomes at 2.3 Å resolution (PDB 4y4o) (15). The designated *stalled ribosome* is colored *slate* and the *trailing ribosome* is colored *gold*, the E-site tRNA is *cyan*, P-site tRNA is *yellow*, and bL9 is *red*. A *pink dashed line* connects the mRNA exit site of the stalled particle to the mRNA entrance of the trailing particle and illustrates the path an extended mRNA would take between those two locations. **B)** In the *left* image, the trailing ribosome was docked in an orientation commonly found in crystals (*collision 1*). 4.4 Å were added to the measured exit-to-entrance distance (64.2 Å in this example) to account for the extra nucleotide on the 5' end of the E-site codon and the resulting distance (68.6 Å) was then divided by 16 Å to obtain a "codon length" of the connecting mRNA (4.3 codons). Finally, four codons were added to account for the mRNA flanking the A-sites in the ribosomes to arrive

at an A-site to A-site spacing in terms of codons to be compared to the experimental data (~8.3 codons in this example). The same codon calculations were performed for the other complexes. Two other packing orientations were found to be compatible with the observed 8-9 codon spacer lengths. In *collision 2*, the trailing particle is rotated ~50 degrees relative to that in *collision 1* such that helix 33 of the trailing small subunit rests on the other side of the uL1 stalk of the stalled ribosome, next to bL9. In *collision 3*, the trailing particle is rotated an additional ~170 degrees and tilted more. In the *collision 2* and *3* complexes, the uL1 stalk contacts the trailing ribosome. **C)** The same operations were performed using cryo-EM structures of *T. thermophilus* ribosomes engaged with the *dnaX* motif (PDB 5uq7) (13). In these, and all other cryo-EM structures, bL9 lies flat against the large subunit and allows the particles in *collision 3* to rest slightly closer together.

SI References

1. Beck HJ & Moll I (2018) Leaderless mRNAs in the Spotlight: Ancient but Not Outdated! *Microbiol Spectr* 6(4).
2. Van Etten WJ & Janssen GR (1998) An AUG initiation codon, not codon-anticodon complementarity, is required for the translation of unleadered mRNA in Escherichia coli. *Mol Microbiol* 27(5):987-1001.
3. Beck HJ, Fleming IM, & Janssen GR (2016) 5'-Terminal AUGs in Escherichia coli mRNAs with Shine-Dalgarno Sequences: Identification and Analysis of Their Roles in Non-Canonical Translation Initiation. *PLoS One* 11(7):e0160144.
4. Parmeggiani A & Sander G (1981) Properties and regulation of the GTPase activities of elongation factors Tu and G, and of initiation factor 2. *Molecular and cellular biochemistry* 35(3):129-158.
5. Deutscher MP (2006) Degradation of RNA in bacteria: comparison of mRNA and stable RNA. *Nucleic Acids Res* 34(2):659-666.
6. Huter P, Muller C, Arenz S, Beckert B, & Wilson DN (2017) Structural Basis for Ribosome Rescue in Bacteria. *Trends Biochem Sci* 42(8):669-680.
7. Amann E, Ochs B, & Abel KJ (1988) Tightly regulated tac promoter vectors useful for the expression of unfused and fused proteins in Escherichia coli. *Gene* 69(2):301-315.
8. OpenWetWare (2015) 'Round-the-horn site-directed mutagenesis. in *OpenWetWare, http://www.openwetware.org*.
9. OpenWetWare (2013) Sauer:bis-Tris SDS-PAGE, the very best. in OpenWetWare, http://www.openwetware.org.
10. Niedermeyer TH & Strohalm M (2012) mMass as a software tool for the annotation of cyclic peptide tandem mass spectra. *PLoS One* 7(9):e44913.
11. Schneider CA, Rasband WS, & Eliceiri KW (2012) NIH Image to ImageJ: 25 years of image analysis. *Nat Methods* 9(7):671-675.
12. Jenner LB, Demeshkina N, Yusupova G, & Yusupov M (2010) Structural aspects of messenger RNA reading frame maintenance by the ribosome. *Nat Struct Mol Biol* 17(5):555-560.
13. Zhang Y, Hong S, Ruangprasert A, Skiniotis G, & Dunham CM (2018) Alternative Mode of E-Site tRNA Binding in the Presence of a Downstream mRNA Stem Loop at the Entrance Channel. *Structure* 26(3):437-445.e433.
14. Zhang J*, et al.* (2015) Mechanisms of ribosome stalling by SecM at multiple elongation steps. *Elife* 4.
15. Polikanov YS, Melnikov SV, Soll D, & Steitz TA (2015) Structural insights into the role of rRNA modifications in protein synthesis and ribosome assembly. *Nat Struct Mol Biol* 22(4):342-344.